Decoherence and relaxation in the interacting quantum dot system

A Letters Journal Exploring the Frontiers of Physics

January 2009

EPL, **85** (2009) 17003
doi: 10.1209/0295-5075/85/17003

www.epljournal.org

Decoherence and relaxation in the interacting quantum dot system

M. Q. Weng[a]

Department of Physics, University of Science and Technology of China - Hefei, Anhui, 230026, China

received 20 October 2008; accepted 24 November 2008
published online 7 January 2009

PACS 72.15.Qm – Scattering mechanisms and Kondo effect
PACS 71.27.+a – Strongly correlated electron systems; heavy fermions
PACS 73.21.La – Quantum dots

Abstract – In this paper we study the low-temperature kinetics of the electrons in the system composed of a quantum dot connected to two leads by solving the equation of motion. The decoherence and the relaxation of the system caused by the gate voltage noise and electron-phonon scattering are investigated. In order to take account of the strong correlation of the electrons in this system, the quasi-exact wave functions are calculated using an improved matrix product states algorithm. This algorithm enables us to calculate the wave functions of the ground state and the low-lying excited states with satisfied accuracy and thus enables us to study the kinetics of the system more effectively. It is found that although both of these two mechanisms are proportional to the electron number operator in the dot, the kinetics are quite different. The noise-induced decoherence is much more effective than the energy relaxation, while the energy relaxation and decoherence time are of the same order for the electron-phonon scattering. Moreover, the noise-induced decoherence increases with the lowering of the dot level, but the relaxation and decoherence due to the electron-phonon scattering decrease.

Introduction. – In the past two decades there have been many experimental and theoretical investigations on the artificial strong interacting quantum system, especially after the observation of the Kondo effect in the quasi–one-dimensional (1D) system composed by a semiconductor quantum dot (QD) connected to two leads. The Kondo effect of this system produces a perfect transparency with unitary conductance in the symmetric configuration $\varepsilon_0 = -U/2$, with ε_0 and U being the QD level and on-site Coulomb repulsion [1–5]. Most of the studies focus on the static transport properties. In recent years, the kinetics and time evolution of these systems also attracted much attention [6–9], as the study of the kinetics and time evolution enables one to attack the strong correlated system from different perspectives. Different methods have been employed to study the response of the systems to the ac-modulated or step switching bias and/or gate voltage [6,10–12]. Theoretically, the temporal evolution of Kondo-like systems has been studied by using noncrossing approximation [6,10,11], quantum Monte Carlo simulation [13], time-dependent numerical renormalization group [14], and time-dependent density matrix renormalization group (DMRG) methods [12]. However, only few studies have considered real dissipation mechanisms, such as noise and the electron-acoustic (AC) phonon interaction, which dominate the decoherence and relaxation at low temperature [15].

In this paper, we study the time evolution of the QD system under the influence of the gate noise and acoustic phonon by solving the equation of motion. Since the electrons in this kind of system are mutually correlated, an improved version of the matrix product states (MPS) algorithm [16–21] is employed to study the electron system in order to keep the many-body effect of the system accurate. The paper is organized as follows. In the second section, we present the system Hamiltonian and the equation of motion for the time evolution of the system in the presence of the gate noise and electron-phonon interaction. In the third section we give a brief introduction to the MPS algorithm and discuss how it can be further improved to study the kinetics of the QD system. We show the numerical results of the decoherence and relaxation in the fourth section and summarize in the last section.

System model. – The system we study is composed of a semiconductor QD connected to two leads. The

[a]E-mail: weng@ustc.edu.cn

Hamiltonian is written as

$$H = H_e + H_{ph} + H_{ep}. \tag{1}$$

Here H_e and H_{ph} are the Hamiltonian of the electron and of the phonon, H_{ep} describes the electron-phonon interaction. The electron Hamiltonian of a N-site system is

$$H_e = \sum_{i\sigma} \varepsilon_i n_{i\sigma} + U n_{0\uparrow} n_{0\downarrow} + \sum_{i\sigma} t_i C^\dagger_{i\sigma} C_{i+1\sigma} + \text{h.c.}, \tag{2}$$

with $C^\dagger_{i\sigma}$ ($C_{i\sigma}$) being the creation (annihilation) operator of the electron with spin $\sigma(=\uparrow\downarrow)$ at the site i. The sites with index $i = 1, 2, \cdots, [N/2](-[N/2], \cdots, -2, -1)$ are the sites on the right (left) lead, while the site with $i = 0$ is for the QD. In this paper, the on-site energy of leads is set to be zero and $t_i \equiv t$ for $i = \cdots, -3, -2, 1, 2, \cdots$. U describes the Coulomb repulsion in the QD. The QD level ε_0 can be controlled by the gate voltage and is subjected to the influence of the noise. For the phonon-related part, we only consider the electron interaction with the background longitudinal AC phonon via deformation potential. The phonon Hamiltonian and the electron-phonon scattering are

$$H_{ph} = \sum_{\mathbf{q}\lambda} \omega_{\mathbf{q}} b^\dagger_{\mathbf{q}} b_{\mathbf{q}} \tag{3}$$

and

$$H_{ep} = \sum_{\mathbf{q}} \sum_{\sigma} n_{0\sigma} M_{\mathbf{q}} (b_q + b^\dagger_{-q}), \tag{4}$$

respectively. $b^\dagger_{\mathbf{q}}$ ($b_{\mathbf{q}}$) is the creation (annihilation) operator of the longitudinal AC phonon with wave vector $\mathbf{q}$, whose frequency is $\omega_{\mathbf{q}} = v_{sl} q$ with v_{sl} standing for the longitudinal sound velocity. $M_{\mathbf{q}} \propto \sqrt{q} \langle \Psi_0 | e^{i\mathbf{q}\cdot\mathbf{r}} | \Psi_0 \rangle$ is the corresponding coupling matrix. Here Ψ_0 is the electron wave function in the dot. It is chosen to have the Gaussian form $\exp(-r^2/2a^2)$ for simplicity, with a denoting the diameter of the QD.

The kinetics of the system is studied by the temporal evolution of the density matrix $\rho(\tau)$, whose diagonal elements $\rho_{n,n}(\tau)$ and off-diagonal ones $\rho_{n,m}(\tau)$ stand for the population of the $|n\rangle$ state and the coherence between $|n\rangle$ and $|m\rangle$ states at time τ, respectively. Here $|n\rangle$ and $|m\rangle$ are the eigen-states of the electron Hamiltonian free from the gate noise and electron-phonon interaction. Using the Markovian approximation and secular approximation, one can write down the equation of motion for the density matrix [22]:

$$\frac{\partial \rho(\tau)}{\partial \tau} = -i[H_e, \rho] - i[H_{LS}, \rho(\tau)] - \sum_{\varepsilon} \Gamma(\varepsilon) \big[n_0(\varepsilon) \times n_0^\dagger(\varepsilon) \rho(\tau) + \rho(\tau) n_0(\varepsilon) n_0^\dagger(\varepsilon) - 2 n_0^\dagger(\varepsilon) \rho(\tau) n_0(\varepsilon) \big]. \tag{5}$$

Here $H_{LS} = \sum_\varepsilon \Delta(\varepsilon) n_0(\varepsilon) n_0^\dagger(\varepsilon)$ is the energy shifting due to the electron-phonon interaction. $\Delta(\varepsilon)$ and $\Gamma(\varepsilon)$ are the real and imaginary parts of the following formula:

$$\Delta(\varepsilon) + i\Gamma(\varepsilon) = \sum_{\mathbf{q}} |M_{\mathbf{q}}|^2 \int_0^\infty \mathrm{d}\tau e^{i\varepsilon\tau} D(\mathbf{q}, \tau), \tag{6}$$

with $D(\mathbf{q}, \tau)$ being the phonon Green function. $n_0(\varepsilon) = \sum_{n,m} \delta_{\varepsilon, E_n - E_m} |n\rangle\langle n|n_0|m\rangle\langle m|$. For the strong electron-optical phonon interaction, H_{LS} plays an important role in the system properties [23]. However, for the weak electron-AC phonon interaction we consider in this paper, it only slightly renormalizes the QD level and the Coulomb interaction, which is hard to detect experimentally. Therefore this shifting is simply omitted in this paper. For the electron-AC phonon interaction via deformation potential $\Gamma(\varepsilon)$ takes the following form:

$$\Gamma(\varepsilon) = \Delta_p |\varepsilon|^3 [(1 + n_B(\varepsilon))\theta(\varepsilon) + n_B(-\varepsilon)\theta(-\varepsilon)], \tag{7}$$

where $n_B(\varepsilon) = 1/(e^{\varepsilon/T} - 1)$ is the Bose function at temperature T, and $\theta(\varepsilon)$ is the Heaviside step function. Δ_p depends on the material- and structure-dependent parameter as well as on the electron-phonon coupling.

Numerical scheme. – To solve the equation of motion, one needs the wave function of the eigen-states of the electron system to obtain the matrix elements of the density matrix and n_0. Since the electrons governed by the Hamiltonian (eq. (2)) form a mutually correlated system, it is important to take the correlation into account in the study of the kinetics at low temperature. Here we use an improved MPS algorithm to obtain the many-body wave functions so that the strong correlation of the electron system can be automatically taken into account.

For the 1D ground-state problem, MPS is known to be equivalent to DMRG [16,17,21]. DMRG was first proposed to study the ground and low-lying excited states of quantum systems [24–26], and later was further extended to the simulation of the time evolution, calculation of excitation spectra and finite-temperature properties of quantum systems [21,27,28]. The success of DMRG is eventually understood by its connection to MPS [16,17,21]. In the MPS algorithm, the wave function of a N-site lattice is represented by a group of A-matrices whose dimension is usually much smaller than the dimension of the Hilbert space

$$\sum_{\substack{s_1 \cdots s_{i-1} \\ s_i s_{i+1} \cdots s_L}} \mathrm{Tr}\big\{ A^{s_1} \cdots A^{s_{i-1}} A^{s_i} A^{s_{i+1}} \cdots A^{s_L} \big\} \times |s_1 \cdots s_{i-1} s_i s_{i+1} \cdots s_L\rangle, \tag{8}$$

with s_i representing the local state index at the i-th site. To start the calculation, an initial wave function is given by other calculations or randomly generated. The wave function is then gradually optimized by a process called "sweep": the wave function is optimized by only minimizing the energy with regard to the local A-matrix at one or two "center" sites while keeping other A-matrices unchanged. One then moves the "center" site to the left or right neighbor by targeting to the ground state [24,25] or performing singular value decomposition [17]. The process repeats until a desirable accuracy is achieved or the accuracy cannot be further improved by more sweeps.

In the traditional DMRG algorithm, if more than one eigen-state are to be calculated, they should be targeted simultaneously during the sweep process. This requires larger A-matrix dimension and more computing resources. The more eigen-states are required, the less accurate they are for a fixed A-matrix dimension. Therefore, the traditional DMRG algorithm is usually limited to the calculation of the ground state and few low-lying excited states. Here we propose an algorithm to improve the calculation of the excited states by using MPS.

In our algorithm, instead of calculating all of the required eigen-states simultaneously, they are calculated step by step. We first calculate the ground state by using the traditional DMRG method and obtain the wave function in the normal MPS form like eq. (8). To obtain the first excited state, we again generate an initial wave function then gradually optimize it through sweep. However, during the sweep, we first orthogonalize the excited state and the ground state by performing Gramm-Schmidt orthogonalization on the local A-matrix at the center site, then we minimize the energy for the excited state. In this way, we can obtain the wave function of the first excited state in the normal MPS form when the sweep converges. Since the wave function of the ground state is in the normal MPS form, the sweep of the first excited state does not change the ground state [29]. Similarly, to calculate the higher excited states, we first perform the orthogonalization of the wave function to all of the lower states, then we optimize the energy during the sweep. By repeating this process, we can get the excited states step by step without sacrificing the accuracy of the lower states.

In our algorithm, the normal MPS form of the wave functions is required to carry out the sweep of the excited states. There are two major algorithms for the sweep: the two-site sweep and the one-site sweep [25,26]. The two-site sweep gives better eigen-energy since it uses a larger Hilbert space and therefore it is more memory hungry and CPU time consuming. Moreover, the wave function obtained by the two-site sweep is no longer in the normal MPS form. For example, if the center sites are $i-1$ and i, the corresponding matrices of the wave function are $\cdots, A^{s_{i-2}}, A^{s_{i-1},s_i}, A^{s_{i+1}}, \cdots$. One has to break the matrix A^{s_{i-1},s_i} into the multiple of two matrices with larger dimension to get the normal MPS form. The wave function loses its optimality if these two matrices are truncated to the original dimension. On the other hand, the one-site sweep is cheaper to carry out. More importantly, the wave function of the one-site sweep algorithm is always in MPS form, therefore it keeps the optimality when the center site moves. However, the one-site sweep can easily fall into some local optimal points and usually fails to give satisfied eigen-energy and wave function unless a good initial wave function is given to start the sweep. Our solution to the dilemma is to use the combination of two-site and one-site sweep. That is, we first use the two-site sweep to improve a randomly generated wave function and truncate the improved wave function to the normal MPS form and use it as the initial wave function for the one-site sweep algorithm. It is expected that the truncated wave function would be a much better initial function even when the initial two-site sweep is not converged.

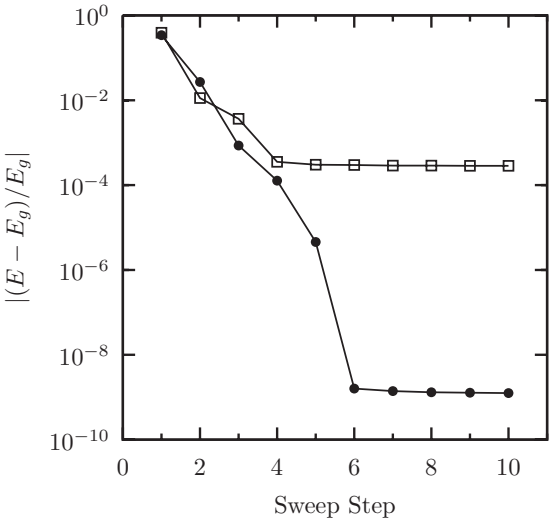

Fig. 1: Relative error of the ground-state energy *vs.* sweep step for the system with $N=17$, and $N_\uparrow = N_\downarrow = 8$. The hopping between the leads and the QD is $0.1t$ and the on-site interaction is $U=6t$. The filled dots are the results of the improved algorithm; the open boxes are those of the single sweep with a randomly generated initial wave function. The curves are guides for the eyes.

In the following we first use this hybrid sweep algorithm to study the ground state of the QD system to demonstrate its feasibility. In fig. 1 the relative error of the ground-state energy is plotted as a function of the number of the sweep. In the calculation, we keep the most relevant 256 states, and the "true" ground-state energy E_g is obtained by the two-site sweep with 400 states kept. In the calculation, the total site number, the spin-up and -down electron number are $N=17$, and $N_\uparrow = N_\downarrow = 8$, respectively. The hopping between the QD and the leads is chosen to be $t_{-1} = t_0 = 0.1t$. In the QD, the on-site energy $\varepsilon_0 = -2t$ and the Coulomb repulsion $U=6t$. For comparison, we also plot the result of the pure one-site sweep with a random initial wave function. It is noted that the first three steps of our new algorithm are a two-site sweep. One can see from the figure that the initial two-site sweep gives a very good start point for one-site sweep even when the initial two-site sweep is not converged. The ground-state energy obtained by this algorithm is very close to that obtained by the two-site sweep. More importantly, with this hybrid sweep algorithm, one not only gets an accurate eigen-energy but also a very accurate wave function with cheaper price. This sweep algorithm also works for the excited states. For higher excited states, the error in the eigen-energy is usually larger than those of the ground state and lower excited states. However, when we keep up to 256 states during the sweep the accuracies of the lowest 10 states are desirable.

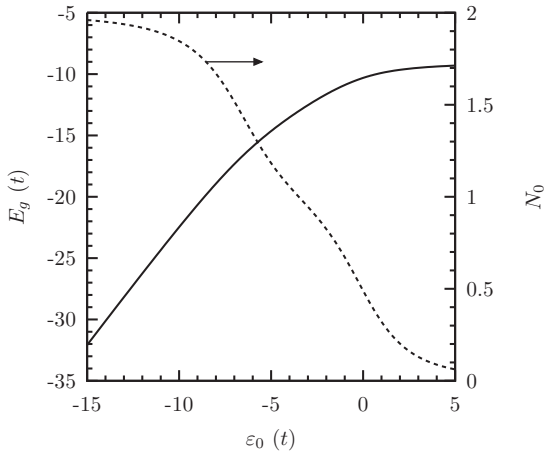

Fig. 2: Ground-state energy E_g (solid curve) and the occupation N_0 (dashed curve) of the QD *vs.* the QD level. Note that the axis for N_0 is on the right. The hopping between the leads and the QD is $0.1t$ and the on-site interaction is $U = 6t$. The site and the electron numbers are $N = 9$, $N_\uparrow = N_\downarrow = 4$, respectively.

We now use this method to calculate the wave functions and the eigen-energies of the system at different gate voltages. The ground-state energy and the electron occupation number in the QD of the system with $N = 9, N_\uparrow = N_\downarrow = 4$ are plotted in fig. 2. One can see that for a positive on-site energy, the electron occupation in the QD is small and the ground-state energy is almost independent of the gate voltage. For a large negative QD level, the QD is doubly occupied and the ground-state energy becomes a linear function of the QD level. The slope of the function is 2, which agrees with the result of $N_0 \simeq 2$. In the regime of $-6t \leqslant \varepsilon_0 \leqslant -2t$, roughly corresponding to the transparent regime ($-U \leqslant \varepsilon_0 \leqslant 0$), it can be seen that the rate of the changing of occupation *vs.* the changing of the QD level is distinctly slower than that of its neighbor. The abnormality in this regime may be related to the formation of a Kondo singlet which is the superposition of the localized and the delocalized states. Since the delocalized states have lower occupation number in the QD, the formation of the Kondo singlet slows down the changing rate of the occupation.

Dephasing and decoherence. – Once we have the wave functions, we can simulate the kinetics of the interacting system under the gate voltage noise and the electron-phonon interaction. In the low-temperature regime, it is expected that only the lowest few states are involved. Therefore we can study the kinetics by solving the equation of motion in the truncated Hilbert space composed of the lowest ten states. We first study the decoherence caused by the noise on the QD level by solving the equation of motion. In the presence of the noise, the QD level becomes $\varepsilon_0 = \bar{\varepsilon}_0 + V(\tau)$, where $\bar{\varepsilon}_0$ is the average QD level, and $V(\tau)$ is the noise due to the fluctuation of the gate voltage. For a system free from noise, the coherence between different states, *i.e.* the off-diagonal elements of

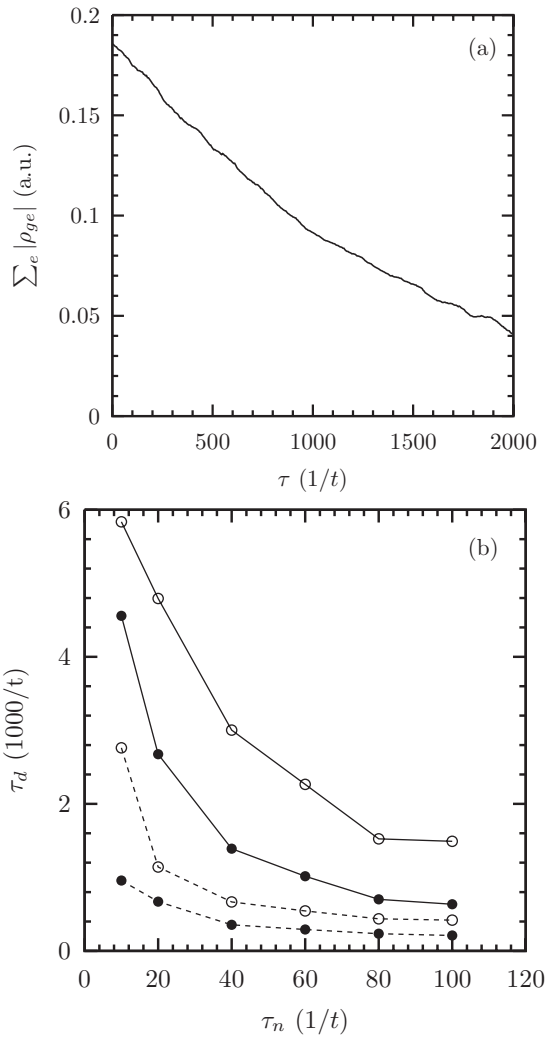

Fig. 3: (a) The temporal evolution of the averaged coherence between the ground state and the excited states for the QD level $\bar{\varepsilon}_0 = -3t$, $\Delta V = 0.5t$ and $\tau_n = 40/t$. (b) The decoherence time as a function of the noise characteristic time τ_n for different situations: solid curves are those for $\Delta V = 0.5t$ and the dashed ones for $\Delta V = 1t$; filled circles and open circles are for $\bar{\varepsilon}_0 = -3$ and $-2t$, respectively.

the density matrix, evolves as $\rho_{n,m}(0)e^{-i(E_n - E_m)\tau}$ whose amplitudes do not decay with time. The noise irregularly shifts the energy levels with different amounts for different states and causes a transition between the states. Since the amplitude of the noise randomly changes, different states eventually lose their phase information over time. As a result the amplitude of the coherence decays with time. In fig. 3(a) we plot the time evolution of the coherence between the ground state and all of the excited states $\sum_e |\rho_{ge}(\tau)|$ under different conditions. To simulate the kinetics of the sudden switch of the gate voltage, the initial wave function is chosen to be the unperturbed wave function of zero gate voltage in the truncated space. The density matrix is averaged over 1000 samplings with the noise $V(\tau)$ evenly distributed over the regime $[-\Delta V, \Delta V]$

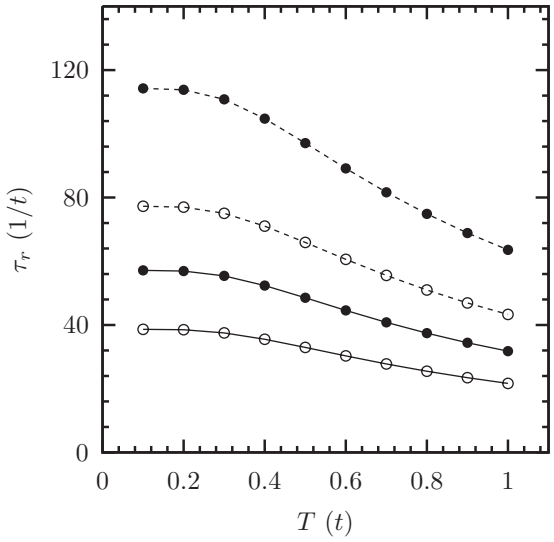

Fig. 4: The relaxation time (solid curves) and the decoherence time (dashed curves) as functions of the temperature T. Filled and open circles are for $\bar{\varepsilon}_0 = -3$ and $-2t$, respectively.

to reflect the randomness of the noise. One can see from the figure that the coherence damped oscillates with time. The envelope of the temporal evolution curve can be fitted by an exponential function $\propto e^{-\tau/\tau_d}$ with a decoherence time τ_d. The decoherence times under different conditions are plotted in fig. 3(b). One can see that the decoherence time decreases with the increase of the noise amplitude and the noise characteristic time τ_n. The on-site energy of the QD also affects the decoherence rate, the higher the QD level the slower the system loses its coherence. The boost of the decoherence rate by the increase of the noise level is quite easy to understand. When the amplitude of the noise increases, the transition rates and the difference of energy shifts become larger. Therefore different states lose the phase information more quickly. The decrease of the decoherence rate with the decrease of τ_n is due to the suppression of the unitary time evolution by the irregular change of the noise. This is similar to the motion narrowing effect [30]. From the Hamiltonian, one can see that the perturbation of the noise is proportional to the electron number in the QD. Therefore, the average QD level also affects the kinetics of the QD system. The lower the QD level, the larger the electron number in the QD, and the smaller the decoherence time. It should be noted that although the gate noise is efficient to remove the phase coherence, it is very inefficient to bring the system to the thermal equilibrium state as it does not directly carry the energy away from the electron system. The relaxation to the thermal equilibrium caused by the noise is more than ten times slower than the decoherence.

We now study the relaxation and decoherence due to the electron-phonon interaction. In fig. 4 we plot the relaxation time τ_r and the decoherence time τ_d as functions of temperature T under different gate voltages. Note that Δ_p is chosen to be t in the calculation. One can see from the figure that both τ_r and τ_d increase as the temperature decreases and saturate at low temperature as the electron-phonon scattering saturates to the emitting phonon limit $\Gamma(\varepsilon) \sim \Delta_p \varepsilon^3 \theta(\varepsilon)$. There are two qualitative differences between phonon-induced relaxation/decoherence and noise-induced relaxation/decoherence, even though their perturbation Hamiltonians are both proportional to n_0, the electron number operator in the QD. Firstly, the phonon-induced relaxation is a little bit faster than the decoherence, while the noise-induced relaxation is more than ten times slower than the decoherence. Moreover, the phonon-induced relaxation and decoherence decrease with the lowering of the QD level. The differences rise from the fact that the electron-phonon scattering is an inelastic scattering. The electron system approaches to thermal equilibrium through an the absorbing or emitting of phonon. As the electron system loses both energy and phase information by the absorbing/emitting of phonon, τ_r and τ_d are of the same order. Furthermore, the main contribution of the n_0 operator to the phonon-induced relaxation/decoherence comes from the off-diagonal elements $n_0(\varepsilon)$ with $\varepsilon \neq 0$. For a lower QD level, the electrons are more deeply trapped in the QD and it is harder for them to hop to higher-energy states. On the other hand, the main contribution of n_0 to the noise-induced decoherence are the diagonal terms, that is the average electron occupation number in the QD. Therefore the lower the QD level, the quicker the noise-induced decoherence.

Conclusion. – In conclusion, we propose an improved matrix product states algorithm to calculate the excited states and use this algorithm to study the relaxation and decoherence caused by the noise and electron-phonon interaction in the interacting QD system. Although both of these two mechanisms are proportional to the electron number operator n_0 in the QD, the kinetics due to these two mechanisms are quite different. The noise shifts the energy with different amounts for different states and causes a transition between the states. The irregular change of the noise results in the losing of the phase information of the electron system and hence of the decoherence. However, the noise does not directly carry energy from the electron system, therefore the energy relaxation due to noise is very inefficient. When the electron-phonon interaction is present, the electron system relaxes to the thermal equilibrium by an absorbing or emitting phonon. As the electron system loses both energy and phase information after the scattering, the energy relaxation and decoherence time are of the same order for the electron-phonon scattering. Moreover, the main effect of the noise comes from the diagonal terms of n_0, while for the electron-phonon scattering it is from the off-diagonal terms. As a result, the noise-induced decoherence increases with the lowering of the QD level, but the relaxation and decoherence due to the electron-phonon scattering decrease.

* * *

The author would like to thank M. W. Wu for the inspiring and valuable discussions. This work is supported by the Natural Science Foundation of China under Grant No. 10804103, the National Basic Research Program of China under Grant No. 2006CB922005 and the Innovation Project of the Chinese Academy of Sciences.

REFERENCES

[1] Ng T. K. and Lee P. A., *Phys. Rev. Lett.*, **61** (1988) 1768.
[2] Glazman L. I. and Raikh M. E., *JETP Lett.*, **47** (1988) 452.
[3] Cronenwett S. M., Oosterkamp T. H. and Kouwenhoven L. P., *Science*, **281** (1998) 540.
[4] Goldhaber-Gordon D., Shtrikman H., Mahalu D., Abusch-Magder D., Meirav U. and Kastner M. A., *Nature*, **391** (1998) 156.
[5] Sasaki S., Franceschi S. D., Elzerman J. M., van der Wiel W. G., Eto M., Tarucha S. and Kouwenhoven L. P., *Nature*, **405** (2000) 764.
[6] Nordlander P., Pustilnik M., Meir Y., Wingreen N. S. and Langreth D. C., *Phys. Rev. Lett.*, **83** (1999) 808.
[7] López R., Aguado R., Platero G. and Tejedor C., *Physica E*, **6** (2000) 379.
[8] Karrai K., Warburton R. J., Schulhauser C., Högele A., Urbaszek B., McGhee E. J., Govorov A. O., Garcia J. M., Gerardot B. D. and Petroff P. M., *Nature*, **427** (2004) 135.
[9] Smith J. M., Dalgarno P. A., Warburton R. J., Govorov A. O., Karrai K., Gerardot B. D. and Petroff P. M., *Phys. Rev. Lett.*, **94** (2005) 197402.
[10] Plihal M., Langreth D. C. and Nordlander P., *Phys. Rev. B*, **61** (2000) R13341.
[11] Plihal M., Langreth D. C. and Nordlander P., *Phys. Rev. B*, **71** (2005) 165321.
[12] Cazalilla M. A. and Marston J. B., *Phys. Rev. Lett.*, **88** (2002) 256403.
[13] Silver R. N., Gubernatis J. E., Sivia D. S. and Jarrell M., *Phys. Rev. Lett.*, **65** (1990) 496.
[14] Anders F. B. and Schiller A., *Phys. Rev. B*, **74** (2006) 245113.
[15] König J., Schoeller H. and Schön G., *Phys. Rev. Lett.*, **76** (1996) 1715.
[16] Östlund S. and Rommer S., *Phys. Rev. Lett.*, **75** (1995) 3537.
[17] Verstraete F., Porras D. and Cirac J. I., *Phys. Rev. Lett.*, **93** (2004) 227205.
[18] Weichselbaum A., Verstraete F., Schollwöck U., Cirac J. I. and von Delft J., arXiv:cond-mat/0504305.
[19] Sørensen E. S. and Affleck I., *Phys. Rev. Lett.*, **94** (2005) 086601.
[20] Hand T., Kroha J. and Monien H., *Phys. Rev. Lett.*, **97** (2006) 136604.
[21] García-Ripol J. J., *New J. Phys.*, **6** (2006) 305.
[22] Breuer H.-P. and Petruccione F., *The Theory of Open Quantum Systems* (Oxford University Press, Oxford) 2002.
[23] Chen Z.-Z., Lü R. and Zhu B. F., *Phys. Rev. B*, **71** (2005) 165324.
[24] White S. R., *Phys. Rev. Lett.*, **69** (1992) 2863.
[25] Noack R. M. and White S. R., *Phys. Rev. B*, **47** (1993) 9243.
[26] Peschel I., Wang X., Kaulke M. and Hallberg K. (Editors), *Density-Matrix Renormalization, A New Numerical Method in Physics* (Springer, Berlin) 1999.
[27] White S. R. and Feiguin A. E., *Phys. Rev. Lett.*, **93** (2004) 076401.
[28] Vidal G., *Phys. Rev. Lett.*, **91** (2003) 147902.
[29] Perez-Garcia D., Verstraete F., Wolf M. and Cirac J., *Quantum Inf. Comput.*, **7** (2007) 401.
[30] Slichter C. P., *Principles of Magnetic Resonance*, 3rd edition (Springer, Berlin) 1996, p. 213.